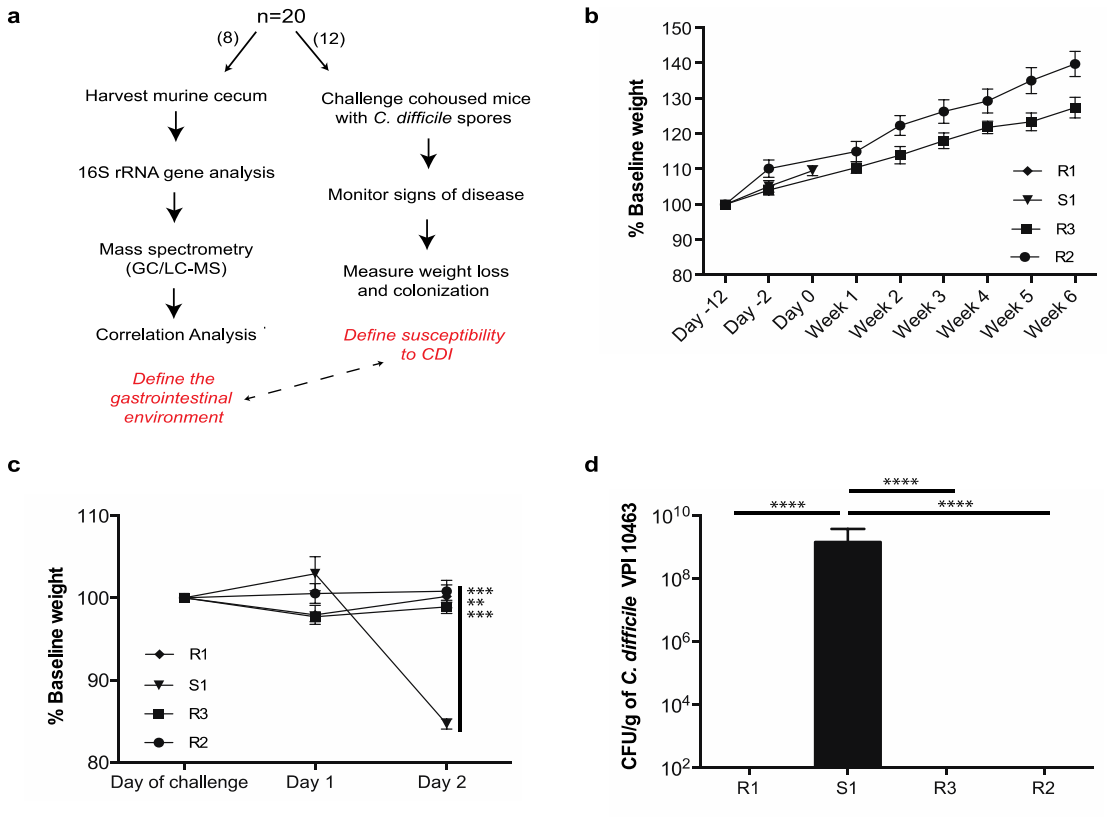

Supplementary Fig. 1: Susceptible and resistant states of *C. difficile* infection
(a) After each treatment and prior to challenge with *C. difficile*, a subset of mice from each group (n=8) were euthanized and cecal content and tissue were collected for microbiome and metabolome analysis. Cohoused mice with the same treatments (n=12) were challenged with *C. difficile* spores to determine susceptibility to CDI. (b) Murine body weight was measured starting the day of cefoperazone treatment (Day -12) and up to 6 weeks after treatment. Solid black lines represent mean percentage of the baseline weight for animals in each group (n=8). All mice gained weight throughout the treatment period. (c) When cohoused mice (n=12) were challenged with *C. difficile* spores the only treatment group that lost a significant amount of weight (d) and were colonized with *C. difficile* were mice from S1. All other treatments were resistant to *C. difficile* infection. Weights were significant for S1 vs. R1, *** p<0.001; S1 vs. R2, *** p<0.001 and S1 vs. R3, ** p<0.01 and colonization was significant for S1 vs. R1, R2 and R3, **** p<0.0001, by non-parametric Kruskal-Wallis one-way analysis of variance test followed by Bonferroni-Dunn Multiple Comparison Test. Error bars represent the mean ± SEM.

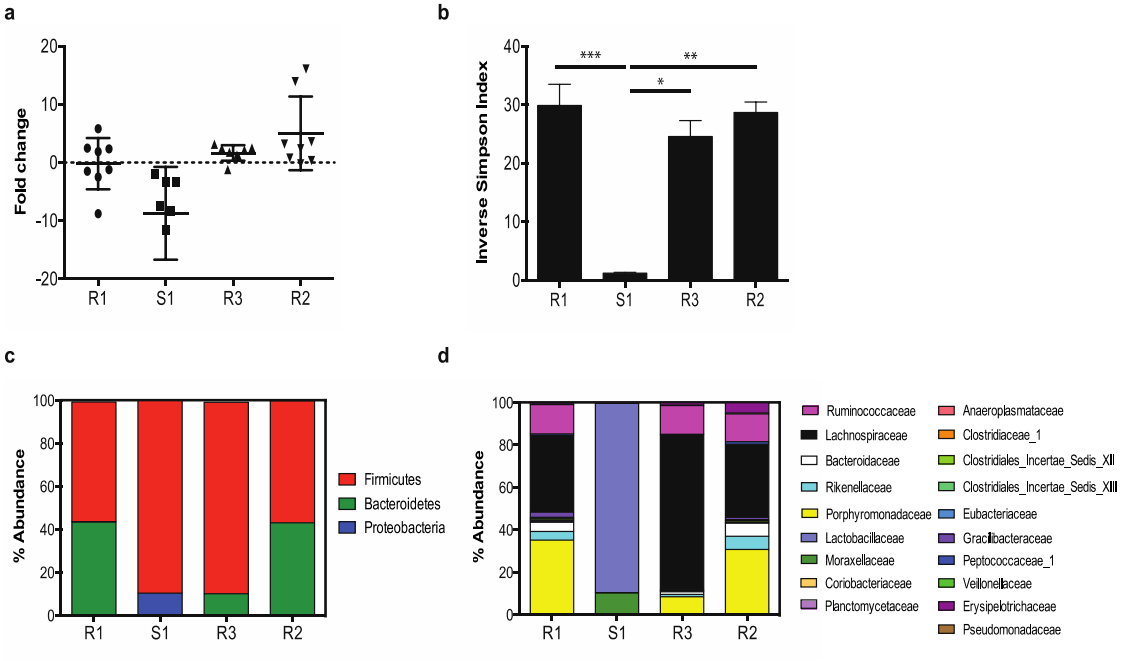

Supplementary Fig. 2: Bacterial load, diversity and membership of the gut microbiome of *C. difficile*-susceptible and -resistant mice

(a) Fold change of the total bacterial load in non-antibiotic and cefoperazone treated mice (each group n=8). There was no significant change in the bacterial load between baseline non-antibiotic treated mice (R1) and all other treatment groups (R1 vs. S1, NS; R1 vs. R3, NS; and R1 vs. R2, NS; by non-parametric Kruskal-Wallis one-way analysis of variance test followed by Bonferroni-Dunn Multiple Comparison Test). Each bar represents the mean ± SD. (b) Bacterial diversity of the cecal microbiota in non-antibiotic and cefoperazone treated mice was measured by the Inverse Simpson Index, which is a measure of alpha-diversity. The S1 mice had significantly less diversity then all other treatment groups (S1 vs. R1, *** $p<0.001$; S1 vs. R3, * $p<0.05$ and S1 vs. R2, ** $p<0.01$ by Kruskal-Wallis one-way analysis of variance test followed by Bonferroni-Dunn Multiple Comparison Test). Each bar represents the mean ± SEM. (c) Defining members of the cecal microbiota by relative rank abundance plots at the bacterial phylum level and (d) the bacterial family level. The average relative abundance for each treatment group (R1 n=7; S1 n=7; R3 n=8; R2 n=8) is represented in the bar plots.

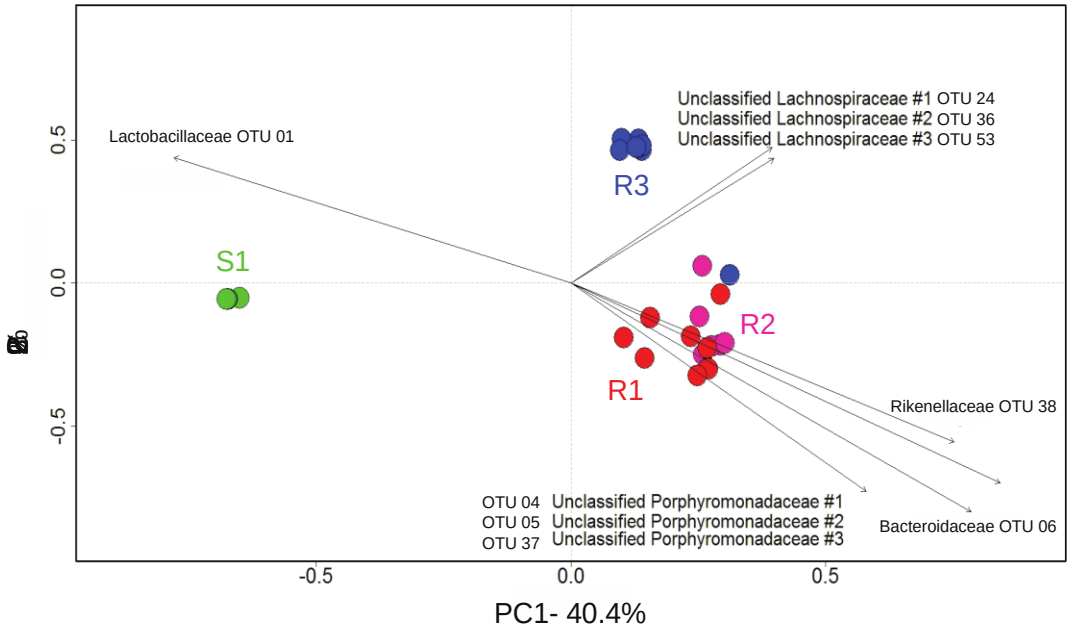

Supplementary Fig. 3: The gut microbiome does not return to baseline 6 weeks after antibiotics, R3

Principle coordinates analysis showed the community structure relationship between non-antibiotic and cefoperazone treated mice. This ordination was generated using a Yue and Clayton-based distance matrix representing the relative abundance of OTUs in each community at a 3% OTU definition level. The community of each mouse is indicated by a colored symbol. Arrows depict how the top nine most frequently detected OTUs influence the location where each mouse is represented. Two days after cefoperazone treatment (S1 in green) the community was driven by OTU1, from the Lactobacillaceae family whereas 6 weeks later (R3 in blue) the community was driven by OTUs from the Lachnospiraceae family. Members of the Porphyromonadaceae, Bacteroidetes and Rikenellaceae family were most abundant in the non-antibiotic treated groups (R1 in red and R2 in pink).

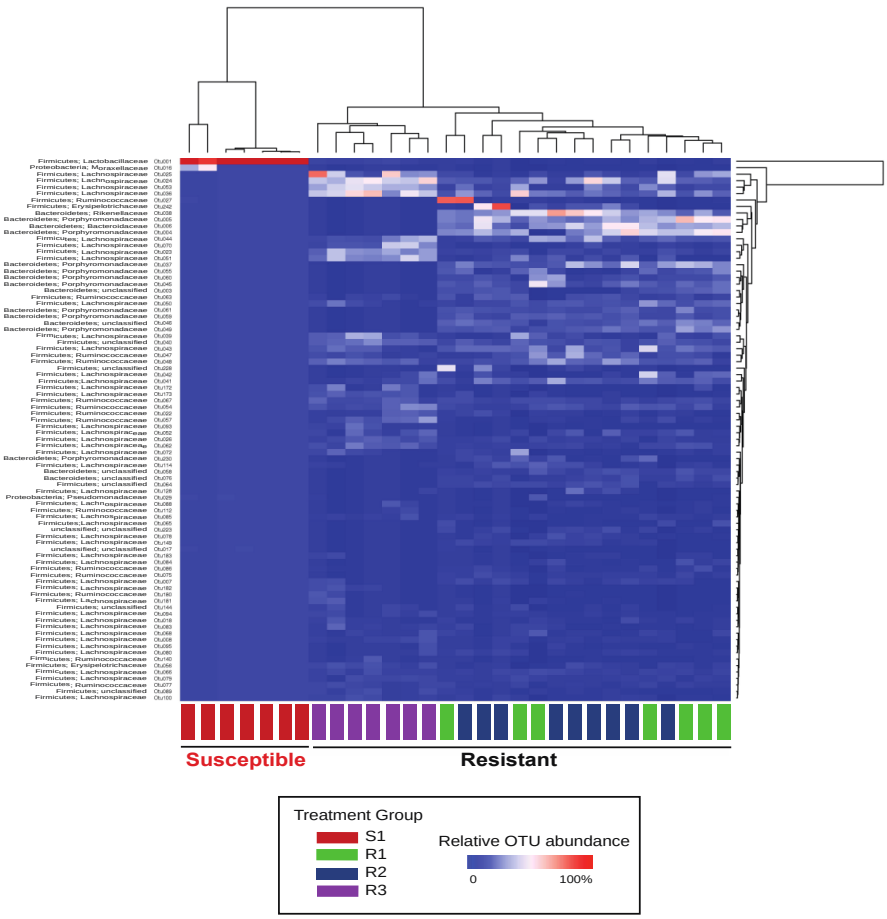

Supplementary Fig. 4: Structural changes to the gut microbiome

A heatmap of the top 84 operational taxonomic units (OTUs) (1% or more of the total sequences) found in the gut microbiome shows differences between CDI susceptible and resistant mice from all four-treatment groups (R1 n=7; S1 n=7; R3 n=8; R2 n=8). The distance between treatment groups was measured by a dendrogram in R statistical program. Two days after stopping cefoperazone (S1 in red bars) mice were susceptible to CDI and group very distinctly from 6-weeks after antibiotic (R3 in purple bars) and non-antibiotic treated mice (R1 in green and R2 in blue bars), which were resistant to CDI. Bacterial phylum, family and OTU number are listed on the heatmap. The heatmap scale ranges from 0 to 100% relative OTU abundance.

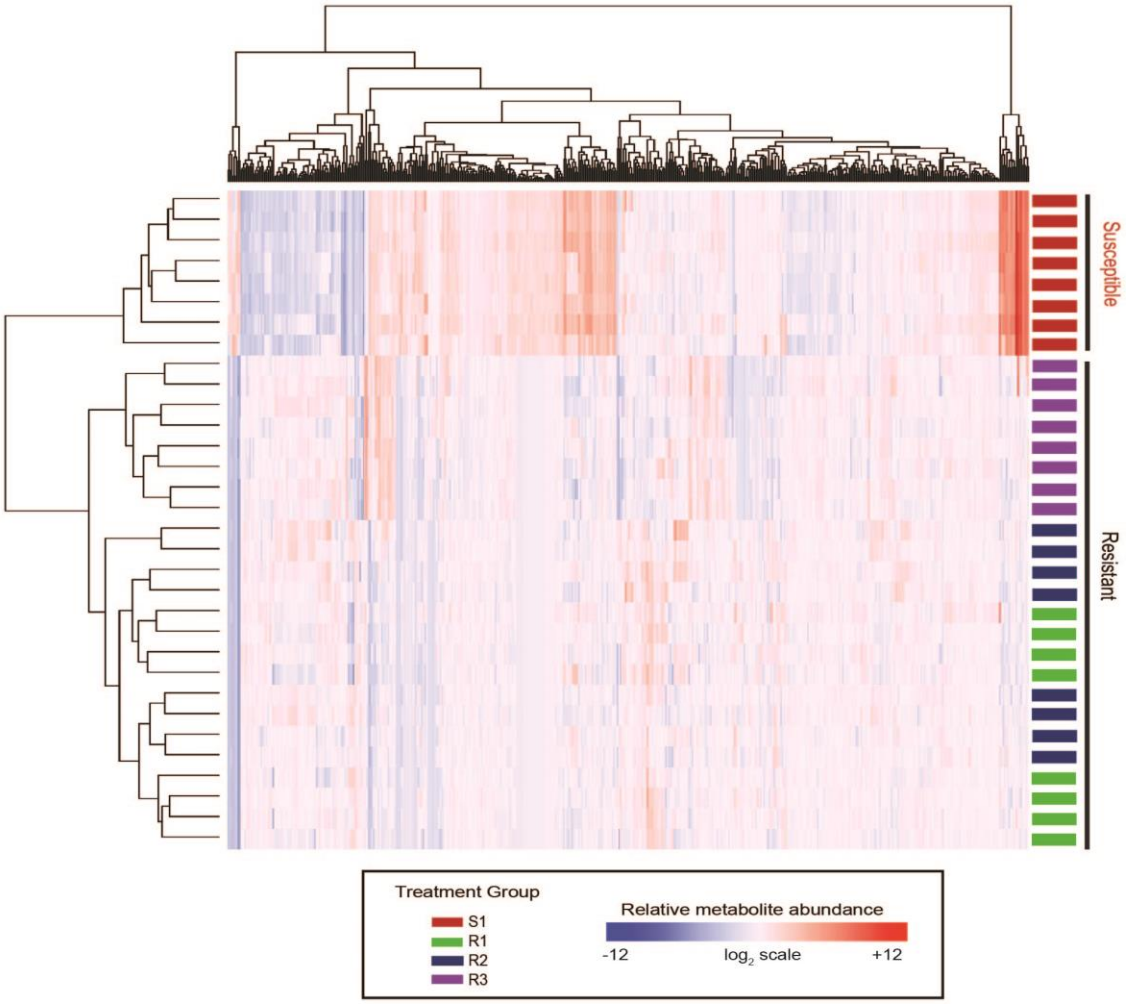

Supplementary Fig. 5: Functional changes to the gut metabolome of *C. difficile*-susceptible and -resistant mice measured by untargeted metabolomics

The cecal content of mice (n=8 for each group) was analyzed by Metabolon, Inc. (Durham, NC) via their platform technology that utilized both GC/MS and LC/MS electrospray positive and negative phases of detection. Raw data was analyzed with R statistical program to generate a heatmap of all 480 metabolites compared to the four treatment conditions with 8 mice per group. The distance between treatment groups was measured and is displayed by a dendrogram in R statistical program. Two days after cefoperazone (S1) the metabolome of mice was significantly different compared to the other three treatment groups (R1-R3) and was also susceptible to CDI. The heatmap scale for relative levels of metabolites ranges from -12 to +12 on a $\log_2$ scale.

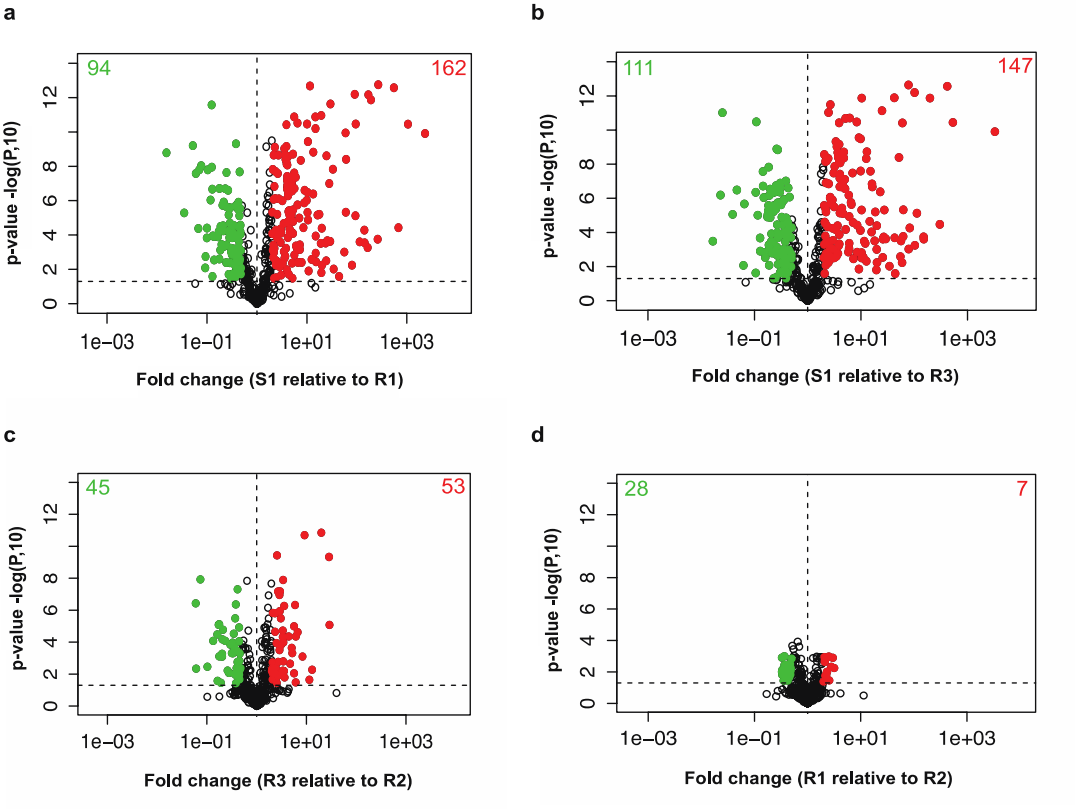

Supplementary Fig. 6: Functional changes to the gut metabolome

Volcano plots, depicting the *p*-value for metabolites on the y-axis and the fold change on the x-axis, were done using R statistical program. Alterations in metabolites during (a) the susceptible state of *C. difficile* infection S1 relative to the non-antibiotic treated resistant state R1. (b) S1 relative to the resistant state 6 weeks after antibiotics R3. (c) Changes in metabolites 6 weeks after stopping antibiotics, R3 relative to non-antibiotic treated mice R2. (d) Changes in metabolites over a 6-week period of non-antibiotic treated mice, R1 relative to R2. Metabolites that increased more than 2-fold and had *p*-value<0.05 by ANOVA are shown in red, while ones that decreased more than 2-fold and had a *p*-value<0.05 are shown in green. The number of metabolites that significantly increased or decreased is listed with in each plot.

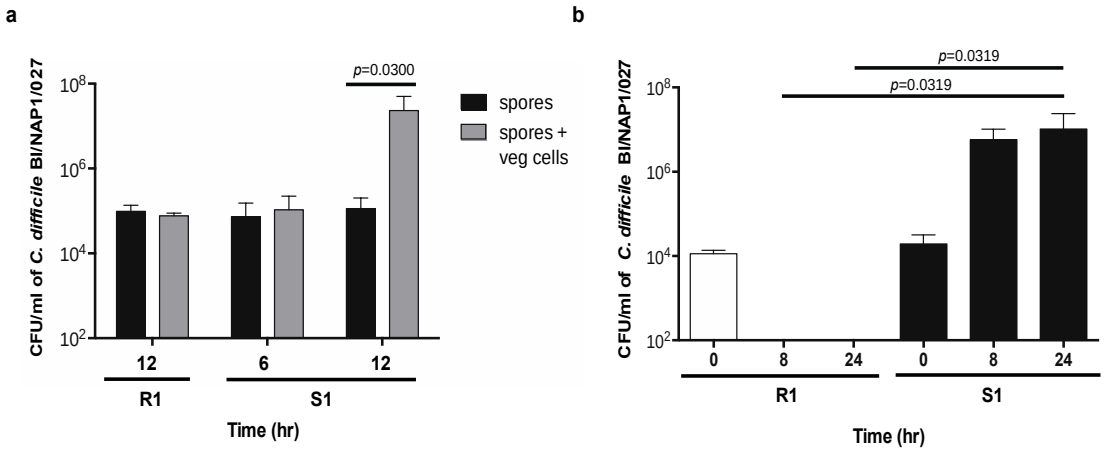

Supplementary Fig. 7: *C. difficile* BI/NAP1/027 *ex vivo* germination and growth studies

(a) *Ex-vivo* germination/outgrowth of *C. difficile* was done in mouse cecal content (non-antibiotic and antibiotic treated). *C. difficile* BI/NAP1/027 spores in the antibiotic treated ceca (S1, n=6) were able to germinate and outgrow over a 6 hour and 12 hour period, whereas spores in the non-antibiotic treated cecal content (n=3) did not. Significance between groups was done by Mann-Whitney non-parametric t-test. Error bars represent the mean ± SEM. (b) *Ex-vivo* growth of *C. difficile* was done in mouse cecal content (R1 and S1). *C. difficile* vegetative cells were able to grow to high levels in the 2 days after cefoperazone treated ceca (S1, n=3) over a 24 hour period compared to non-antibiotic treated ceca (R1, n=3). Data presented represent mean ± SD of triplicate experiments and were significant by non-parametric Kruskal-Wallis one-way analysis of variance test followed by Bonferroni-Dunn Multiple Comparison Test.

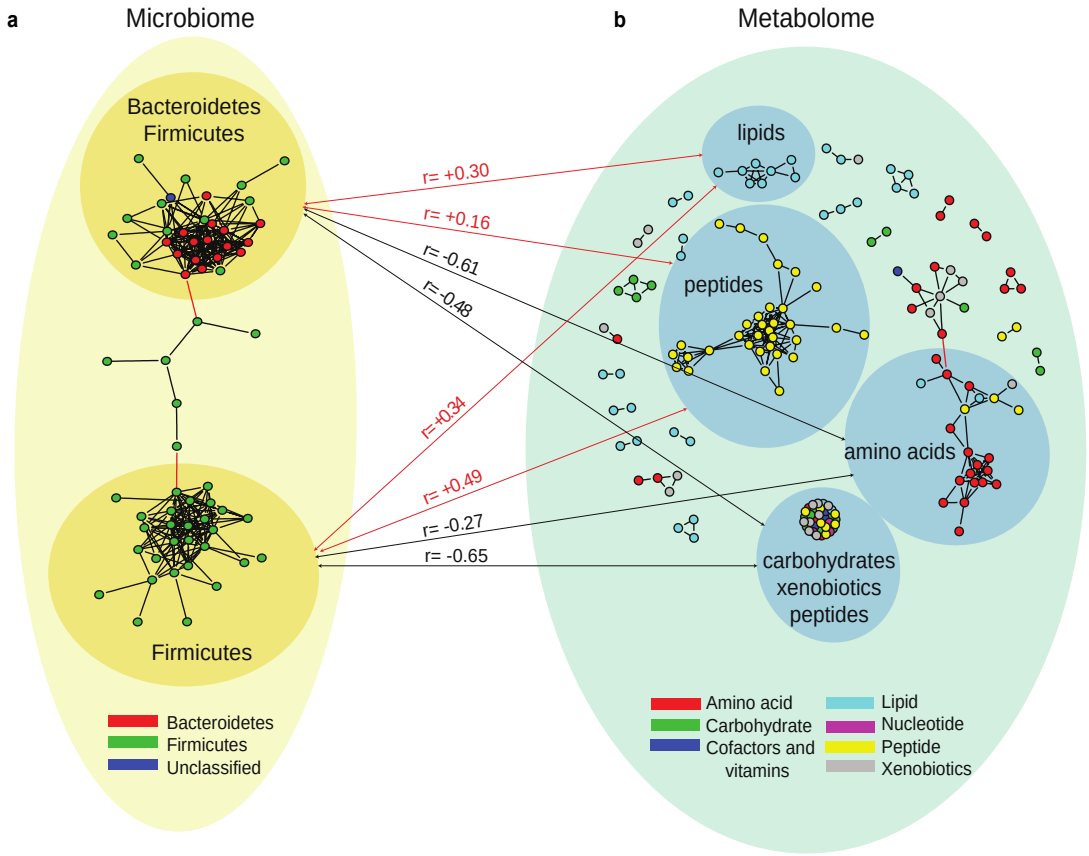

Supplementary Fig. 8: Network analysis between the microbiome (a) and metabolome (b)

The OTUs in (a) aggregate into two networks, one dominated by Firmicutes and another with a mix of Bacteroidetes and Firmicutes whereas the network of metabolites in (b) contain dense clusters that correspond to lipids, peptides, amino acids, carbohydrates and xenobiotics. Spearman's correlation matrix was done between the 157 metabolites and the 63 OTUs, to explore how each group of metabolites was affected by the OTUs. The arrows represent positive (red) or negative (black) correlations between clusters of OTUs ad metabolites, with the r-value representing the Spearman's rank correlation coefficient. Individual OTUs and metabolites are depicted as nodes with a legend displaying the color with the corresponding phylum and the KEGG super pathway designation.

Supplementary Table 1: *C. difficile* growth rates with carbohydrates *in vitro*

Carbohydrate	Growth rate (μ)
Sorbitol	0.62 ± 0.06
Mannitol*	0.66 ± 0.10
Arabitol	0.58 ± 0.09
Xylitol	NA
Gluconate	0.54 ± 0.01
Sucrose	0.52 ± 0.04
Lactate	0.55 ± 0.05
Raffinose	0.56 ± 0.03
Stachyose	0.55 ± 0.03
Galactose	NA
Fructose*	0.66 ± 0.12
Glucose control*	0.73± 0.09
Amino Acids, No Carbohydrates	0.54 ± 0.02
No Amino Acids, No Carbohydrates	NA

Growth rates (in $hours^{-1}$) are shown. *C. difficile* was grown in defined minimal media supplemented with various carbon sources (5 mg/ml). Values given are the growth rates from three independent cultures. *denotes carbohydrates that had significant growth rates compared to Amino Acids, No Carbohydrates control. Data presented represent mean ± SD of triplicate experiments and were significant by ANOVA one-way analysis of variance test followed by Bonferroni-Dunn post-test. NA: Not applicable because no growth was observed.